



HAL
open science

New Promising Modified Activated Carbons for CH₄ and CO₂ Adsorption

G. Iragena Dushime, J. Bachelart, K. Abou Alfa, C. Matei Ghimbeu, Cecile Hort, V. Platel

► **To cite this version:**

G. Iragena Dushime, J. Bachelart, K. Abou Alfa, C. Matei Ghimbeu, Cecile Hort, et al.. New Promising Modified Activated Carbons for CH₄ and CO₂ Adsorption. *Journal of Environmental Science and Engineering. A*, 2023, *Environmental Science and Engineering*, pp.151-163. 10.1007/978-981-19-9440-1_12 . hal-04490693

HAL Id: hal-04490693

<https://univ-pau.hal.science/hal-04490693>

Submitted on 5 Mar 2024

HAL is a multi-disciplinary open access archive for the deposit and dissemination of scientific research documents, whether they are published or not. The documents may come from teaching and research institutions in France or abroad, or from public or private research centers.

L'archive ouverte pluridisciplinaire **HAL**, est destinée au dépôt et à la diffusion de documents scientifiques de niveau recherche, publiés ou non, émanant des établissements d'enseignement et de recherche français ou étrangers, des laboratoires publics ou privés.

Query Details

[Back to Main Page](#)

1. Please check and confirm if the author names and initials are correct.

New Promising Modified Activated Carbons for CH₄ and CO₂ Adsorption

G. Iragena Dushime ✉

Email : grace.iragena-dushime@univ-pau.fr

Affiliationids : Aff1, Correspondingaffiliationid : Aff1

J. Bachelart Affiliationids : Aff1

K. Abou Alfa Affiliationids : Aff1

C. Matei Ghimbeu Affiliationids : Aff2

C. Hort Affiliationids : Aff1

V. Platel Affiliationids : Aff1

Aff1 Université de Pau et des Pays de l'Adour/E2S UPPA, Laboratoire de Thermique, Energetique Et Procèdes, EA1932, 64000, Pau, France

Aff2 Institut de Sciences des Matériaux de Mulhouse, CNRS UMR 7361 UHA, 15 Rue Jean Starcky, 68057, Mulhouse, France

Abstract

This work focuses on **AQ1** methane (CH₄) and carbon dioxide (CO₂) pure gases adsorption using commercial activated carbon (CNR-115), and its modified activated carbons: the one obtained via oxidation (CNR-115-ox) and the other given by oxidation followed by ammonium impregnation (CNR-115-ox-am). A homemade setup was used for isotherms determination at 303.15 K and 0–3 MPa. At 3 MPa, CO₂ and CH₄ uptakes were: CNR-115 (12.05 and 5.18 mmol/g respectively) > CNR-115-ox (7.79 and 3.16 mmol/g respectively) > CNR-115ox-am (4.05 and 1.53 mmol/g respectively). Hence: (a) CNR-115 with high BET surface area (1714 m²/g) adsorbs higher amount of gases than CNR-115-ox (929 m²/g), which also adsorbs more gases than CNR-115-ox-am with the least BET surface area (352 m²/g), and (b) CO₂ with smaller molecular size (330 pm) is more adsorbed on activated carbons surface than CH₄ (380 pm). Further, the Langmuir model was used for adsorption description and the results are well comparable to the ones reported in the literature. Lastly, an interesting side of CNR-115-ox-am was discussed, and this activated carbon was found to be promising for CH₄ enrichment from CH₄/CO₂ mixtures due to its low CH₄ uptake.

Keywords

Activated carbons
Adsorption
Carbon dioxide
Methane

12.1. Introduction

The global world climate change and energy sector development are two main keys factors to promote the use of renewable energies. Historically, the use of gas for energy production began at the end of the nineteenth century. The sector was then improved and underwent many transformations (Gasquet [2020](#)). Indeed, the first-generation gas called the city gas was obtained from coal pyrolysis and was then replaced by natural gas due to the fact that, the latter is naturally formed in some porous rocks and extracted by drilling instead of pyrolysis which also requires the use of energy. Currently, biogas (i.e. the third generation gas) is gaining too much attention over coal and natural gas because the former is a renewable energy contributing in climate protection by reducing the emissions of greenhouse gases such as carbon dioxide (CO₂) (Vondra et al. [2019](#)). Biogas (i.e. The mixture of CH₄ (30–75%) and CO₂ (15–50%)) is produced from a process called anaerobic digestion through biochemical degradation of organic wastes materials (Boulinguez and Cloirec [2015](#)). However, the presence of carbon dioxide is not crucial for the use of biogas, as it lowers its heating value. This is the main reason of upgrading the biogas in order to produce biomethane which can therefore be used: (i) for energy production, ii) as fuel for vehicles, and iii) natural gas pipelines injection. Concerning pipelines injection of biomethane, the gas must fit pipelines-quality requirements (i.e. CO₂ < 3%, and CH₄ > 97%) (Olivier [2015](#)). Biomethane is almost similar to natural gas in terms

between them is based on CO₂ emissions. For example, since 2017 the direct emissions of carbon from biomethane in France (23 gCO₂/kWh) was about ten times less than the one from natural gas (244 gCO₂/kWh) (Gasquet [2020](#)), this explains the reason to prefer biomethane than natural gas. However, the price of biomethane in France (~100 €/MWh) is still higher compared to the price of natural gas (<20 €/MWh) (Tilagone and Lecointe [2015](#)), this is why many researches are increasingly conducted dealing with ways to reduce this price. Reducing the costs of biogas upgrading is one of ways to reduce the biomethane price. This work highlights the role of activated carbons (ACs) in biogas upgrading. Different technologies are known for biogas upgrading: Pressure Suing Adsorption (PSA), water scrubbing, amine scrubbing, membrane, cryogenic, and biological treatments. However, some of those technologies are pricey, others are energivores, and others emit chemicals enhancing climate-damaging. PSA technology is preferred due to its low costs and low energy requirements (Kapoor et al. [2019](#)). Moreover, PSA is based on the use of solid adsorbent materials such as activated carbons, zeolites, and metal organic frameworks to remove CO₂ via adsorption process; this makes it applicable over a wide range of temperatures and pressures (Speight [2019](#)). Among adsorbents for CO₂ removal, activated carbons are considered as the best, thanks to their good textural properties, their good stability under acidic and basic conditions (El-Shafey et al. [2016](#)), their low costs, and their ease of regeneration (Pu et al. [2021](#)). ACs dispose high specific surface areas (400–3500 m²/g) and large pores sizes (1.0–4.0 nm) (Sun et al. [2016](#)), leading to high CO₂ adsorption capacity but low selectivity (Ribeiro et al. [2008](#)). However, the selectivity of activated carbons can be optimized through surface modification (i.e. introducing chemical or/and physical materials) (Zulkurnai et al. [2017](#)). This work provides insight regarding the influence of activated carbons modification on CH₄ and CO₂ adsorption. For that concern, a homemade manometric setup was used, and a sufficient number of experiments were conducted on the adsorption of pure gases (CH₄ and CO₂) by commercial CNR-115 and two new modified activated carbons (CNR-115-ox and CNR-115-ox-am) at 303.15 K and the pressure range of 0–3 MPa. To describe the behavior of CH₄ and CO₂ on a set of activated carbons used, the Langmuir two parameters model was used and the results are well comparable to the ones are well comparable to the ones in the literature.

12.2. Materials and Methods

12.2.1. Commercial and New Modified Activated Carbons (Family of CNR-115)

Three activated carbons used in this work: commercial (CNR-115) and two new modified (CNR-115-ox and CNR-115-ox-am) were purchased at Mulhouse Materials Science Institute (IS2M, France). The surface chemistry of commercial CNR-115 was modified through two successive steps: (a) oxidation under air at 400 °C for 2 h to increase the number of oxygenated groups. Activated carbon produced in this step is called CNR-115-ox, and (b) ammonium vapor (NH₄OH) impregnation at 298 K for 36 h to increase the amount of nitrogenated groups. The resulted activated carbon in this step is called CNR-115-ox-am.

12.2.2. Activated Carbons Characterization

Textural properties of activated carbons were characterized by means of nitrogen adsorption/desorption measurements using a micromeritics ASAP2020 under 77 K. BET (Brunauer, Emmet and Teller) model was used for specific surface area (SSA) determination. The total pore volume (V_t) was obtained for P/P₀ equals to 0.99. Dubinin-Radushkevich model was used to calculate the micropore volume (V_{micro}), whereas the mesopore volume (V_{meso}) was given by the difference between V_t and V_{micro}. SAIEUS software (Micromeritics) and 2D-NLDFIT (Non Local Density Functional Theory (Jagiello and Olivier [2013](#))) were applied to determine the pore size distribution (PSD) which served in the average pore width (L₀) determination through the Eq. ([12.1](#)).

$$L_0 = \frac{1}{N} \sum_{i=1}^N \frac{w \cdot dV/dW}{dV/dW} \quad 12.1$$

where L_0 is the average pore diameter (nm), w is the pore width (nm), dV/dW is the differential pore volume per pore width (cm³ nm⁻¹), and N is the number of data points. The Table [12.1](#) presents the textural properties obtained for activated carbons of the CNR-115 family: CNR-115, CNR-115-ox and CNR115-ox-am. In the Table [12.1](#), it can be observed that the surface modification process remarkably reduces the BET surface of activated carbons of the CNR-115 family in the following sequence: CNR-115 (1714 m² g⁻¹) > CNR-115-ox (929 m² g⁻¹) > CNR-115-ox-am (352 m² g⁻¹). The total pore volume has also decreased (more than half) after each modification process: CNR-115 (0.95 cm³ g⁻¹) > CNR-115-ox (0.45 cm³ g⁻¹) > CNR-115-ox-am (0.21 cm³ g⁻¹). Micro and meso-pore volumes, and average pore size were also impacted. However, the decrease in BET surface area is considered as normal result of modification process due to the fact that, the latter includes the temperature rise and thus the mass vaporization. The decrease in porosity can be associated with pore blockage that takes place during modification where the loading of oxygen and nitrogen functional groups may block some pores (Madzaki et al. [2016](#)).

Table 12.1

Textural properties of CNR-115, CNR-115-ox and CNR115-ox-am (Peredo-Mancilla et al. [2018](#))

Activated carbon	S_{BET} (m^2g^{-1})	V_{micro} (cm^3g^{-1})	V_{meso} (cm^3g^{-1})	V_{tot} (cm^3g^{-1})	L_0 (nm)
CNR-115	1714	0.64	0.31	0.95	1.10
CNR-115-ox	929	0.36	0.09	0.45	0.96
CNR-115-ox-am	352	0.14	0.07	0.21	0.78

On the other hand, the N_2 adsorption/desorption and 2D-NLDFT pore size distribution (Figs. [12.1](#) and [12.2](#) respectively) behave as type I isotherm because: (i) the adsorbed volume increases at low pressures, and (ii) there is the plateau formation at higher pressures.

Fig. 12.1

N_2 adsorption/desorption of CNR-115, CNR-115-ox and CNR-115-ox-am (Peredo-Mancilla et al. [2018](#))

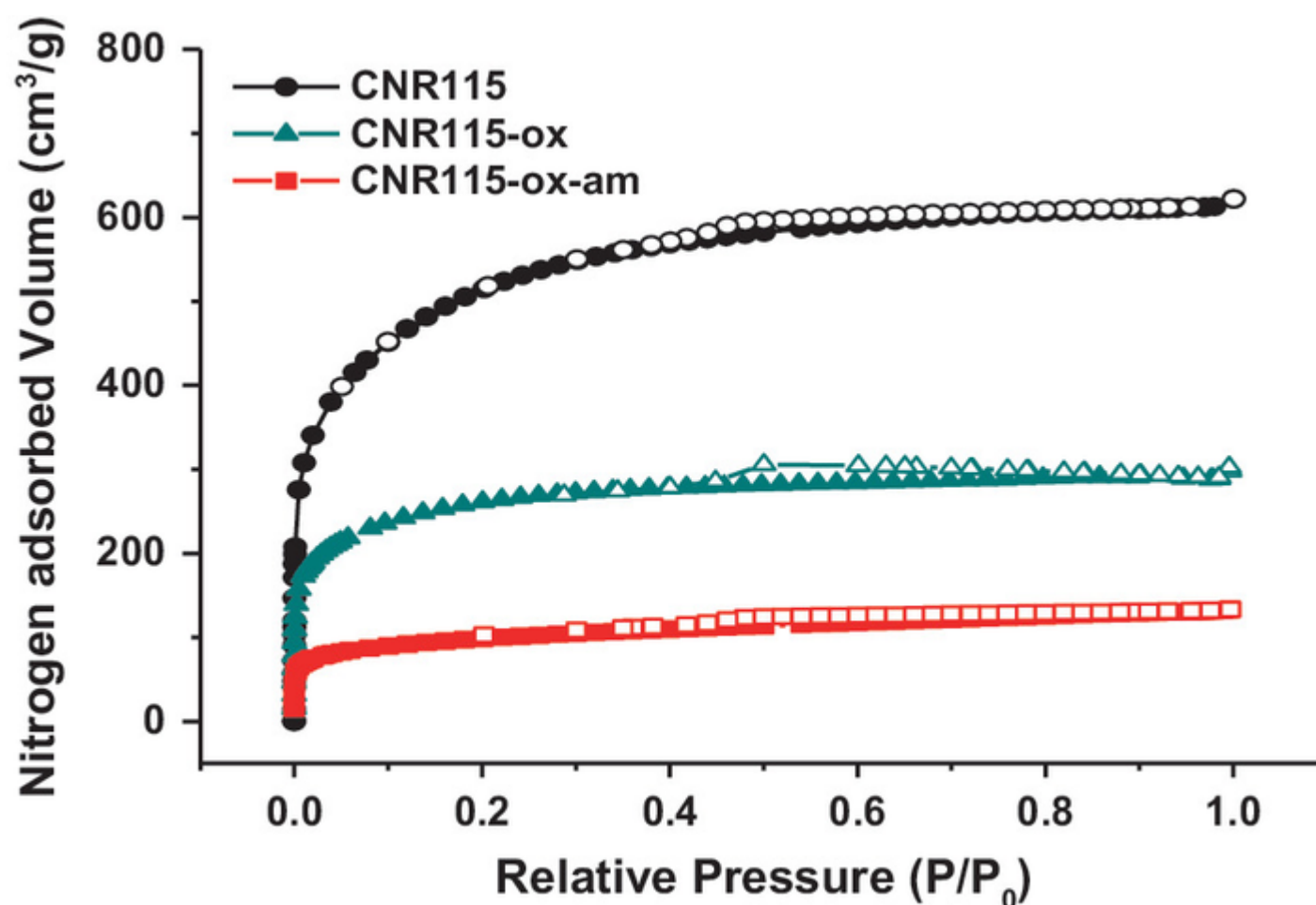
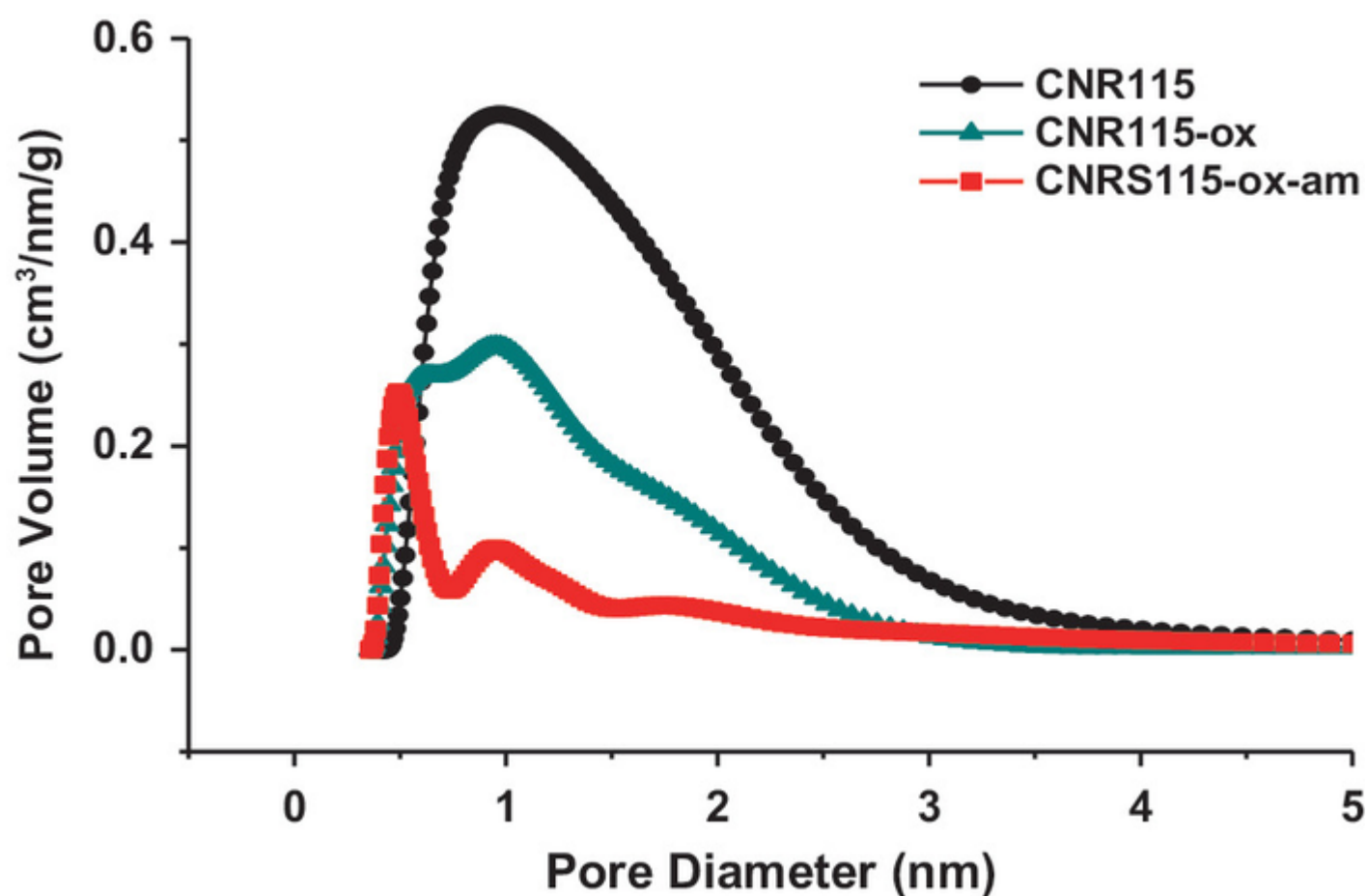


Fig. 12.2

Pore size distribution of CNR-115, CNR-115-ox and CNR-115-ox-am (Peredo-Mancilla et al. [2018](#))

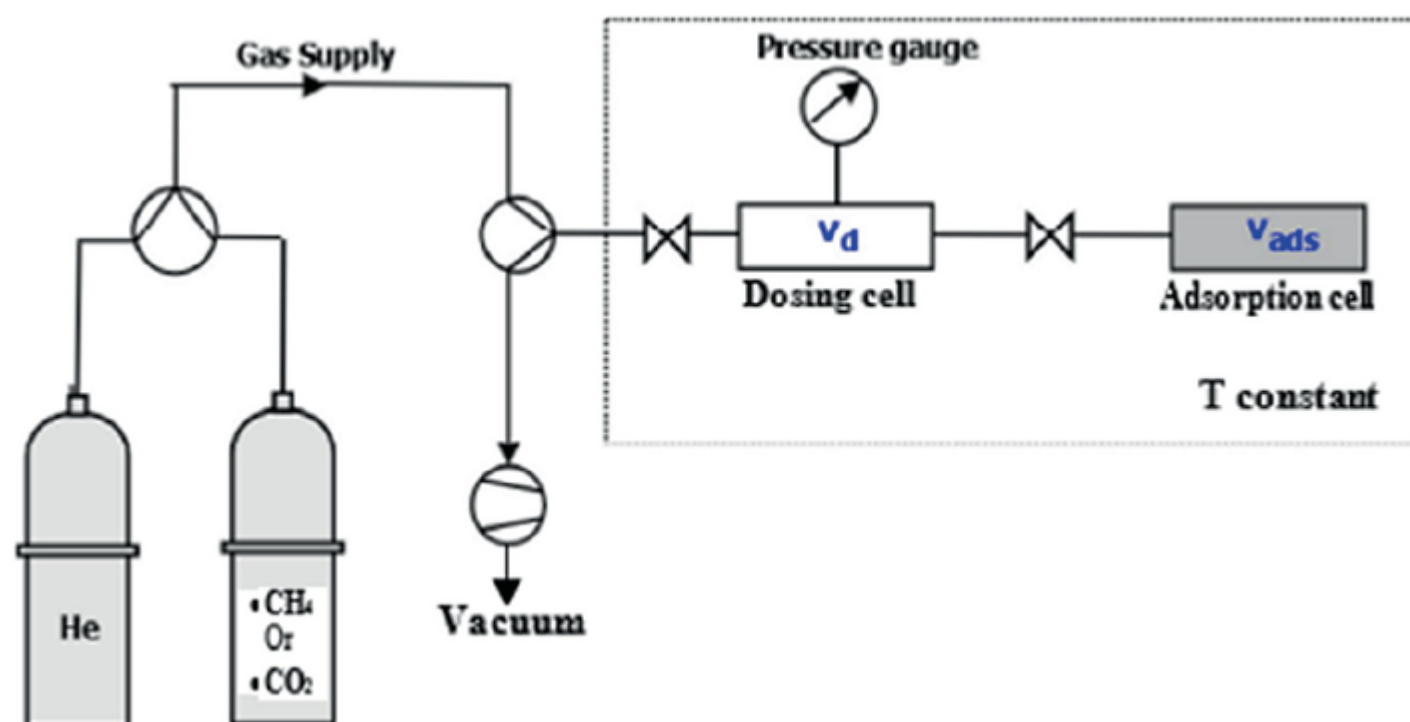


12.2.3. Experimental System

Adsorption isotherms were determined by using manometric setup presented on the Fig. 12.3, at the temperature of 303.15 K and the pressure range of 0–3 MPa.

Fig. 12.3

High-pressure manometric device for pure gases adsorption (adapted from Peredo Mancilla 2019)



The system is composed of two basic elements which are the dosing and adsorption cells. To measure the pressure inside the cells, MKS pressure transducer baratron type 121 A (with 0.01% uncertainty from vacuum to 3.3 MPa) was used. The dosing and adsorption cells are separated by valves, whose also allow minimizing the dead space volume. Isothermal condition of the system was maintained at 303.15 K by wrapping the cells with a heating wire controlled by a Eurotherm 3208 PID regulator, and was verified by using two thermocouples fixed on the cells. The system is also connected to the vacuum pump for regeneration process.

12.2.4. Volume Calibration

The dosing and adsorption cell volumes of the empty system were previously calculated by Deneb et al. (Peredo Mancilla 2019) by means of gravimetric calibration method, and the values obtained were 30.8 and 19.05 cm³ for dosing and adsorption volumes respectively. Determination of the volume occupied by adsorbent is then the preliminary step which must be done once a new mass of adsorbent sample is introduced into the system. This volume is slightly different from the one of the empty cell due to the fact that, the small volume is occupied by adsorbent. To do so, a small amount of activated carbon (~1 g) was placed inside the adsorption cell (after vacuum at 90 °C for 8 h). When the isothermal conditions at the experimental temperature (303.15 K) was reached, the small pressure of helium gas (i.e., inert gas which is not adsorbed by activated carbons) was introduced into the dosing cell. After the pressure stabilization, the initial pressure (P_i^i) was noted and the gas was expanded into the whole system (Bessières et al. 2005). At that stage, when the new stabilization of pressure was obtained, the final pressure (P_f^i) was taken and the first point ($i = 1$) of the dead space volume (V_m) of adsorption cell was calculated by means of the ideal gas equation of state using the Eq. (12.2). Other doses of helium were then introduced successively in the dosing cell and expanded into the adsorption cell. The dead-space volume for the i th step was therefore expressed by using the Eq. (12.3), and the final dead space volume was given by the average of all the measurements.

$$V_m = V_d \left(\frac{P_i}{P_f} - 1 \right) \quad 12.2$$

$$V_m^i = V_d \left(\frac{P_i^i - P_f^i}{P_f^i - P_f^{i-1}} \right) \quad 12.3$$

12.2.5. CH₄ and CO₂ Pure Gases Adsorption Measurements

To determine CH₄ and CO₂ pure gases adsorption isotherms, the main steps of experimental methodology are the following: (i) a small activated carbon sample was measured and introduced directly into the adsorption cell. In this work, the amount of around 1 g was chosen in order to get enough available adsorption area (50 m² is the minimum surface required) (Mouahid et al. 2011). (ii) The experimental system was regenerated under vacuum at 90 °C for 8 h in order to remove all the gases fixed at the surface of activated carbon. (iii) The third step is to calculate the volume occupied by the adsorbent (as detailed above). (iv) The experimental temperature (303.15 K) was then settled. (v) Lastly, the successive doses of gas (CH₄ or CO₂) were introduced and expanded into the dosing and adsorption cells respectively, and the initial and final pressures were noted after reaching the equilibrium. The number of adsorbed moles for the first point of the adsorption isotherm (n_{ads}^1) was calculated by using the Eq. 12.4, and the others points of the adsorption isotherm (n_{ads}^i) were given by the Eq. (12.5).

$$n_{\text{ads}}^1(T, P_1) = (V_d \rho_i) - ((V_d + V_m) \rho_f) \quad 12.4$$

$$n_{\text{ads}}^i(T, P_i) = (V_m \rho_f^{i-1} + V_d \rho_i^i) - ((V_d + V_m) \cdot \rho_f^i) \quad 12.5$$

where ρ_i and ρ_f (g cm^{-3}) are the molar density at initial and final pressures respectively. The values of ρ_i and ρ_f at the experimental temperature and pressures conditions were taken from the NIST (National Institute of Standards and Technology) database.

12.2.6. Langmuir Fitting Model

To study the adsorption behavior of pure CH_4 and CO_2 on the mentioned adsorbents, Langmuir two-parameter model (which takes into account the adsorbed phase) was used as in Eq. (12.6) (Ortiz Cancino et al. 2017).

$$n_{\text{ads}}^{\text{excess}} = n_L \frac{P}{P + P_L} \left(1 - \frac{\rho_g(P, T)}{\rho_{\text{ads}}} \right) \quad 12.6$$

where $n_{\text{ads}}^{\text{excess}}$ (mol kg^{-1}) is the amount of gas adsorbed at the working pressure P (MPa), P_L (MPa) is the Langmuir pressure, ρ_g (kg m^{-3}) is the gas density, and ρ_{ads} (kg m^{-3}) is the adsorbed phase density. In this work, the values of ρ_{ads} are fixed to be 1027 kg m^{-3} and 423 kg m^{-3} for CO_2 and CH_4 respectively (Ortiz Cancino et al. 2017). The error of the fitting process (Δ_n) was calculated through the standard deviation between experimental number of adsorbed moles and theoretical ones as in the Eq. (12.7).

$$\Delta_n = \frac{1}{N} \cdot \sqrt{\sum_{i=1}^N (n_{\text{ads}}^{\text{exp}} - n_{\text{ads}}^{\text{FIT}})^2} \quad 12.7$$

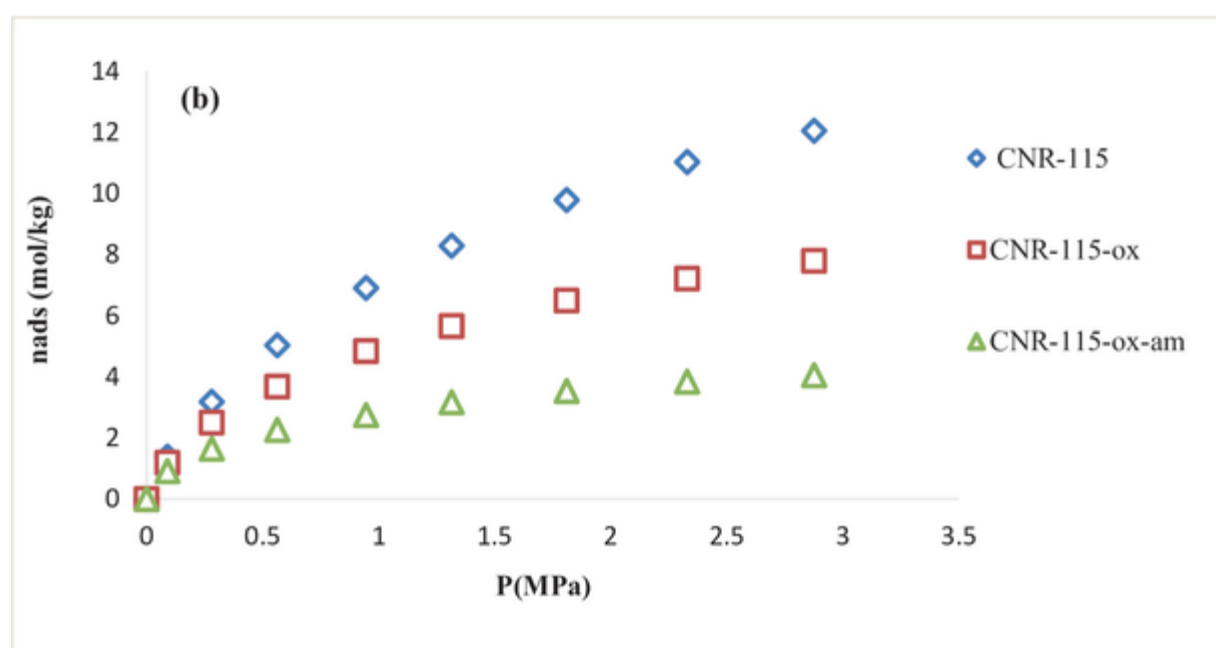
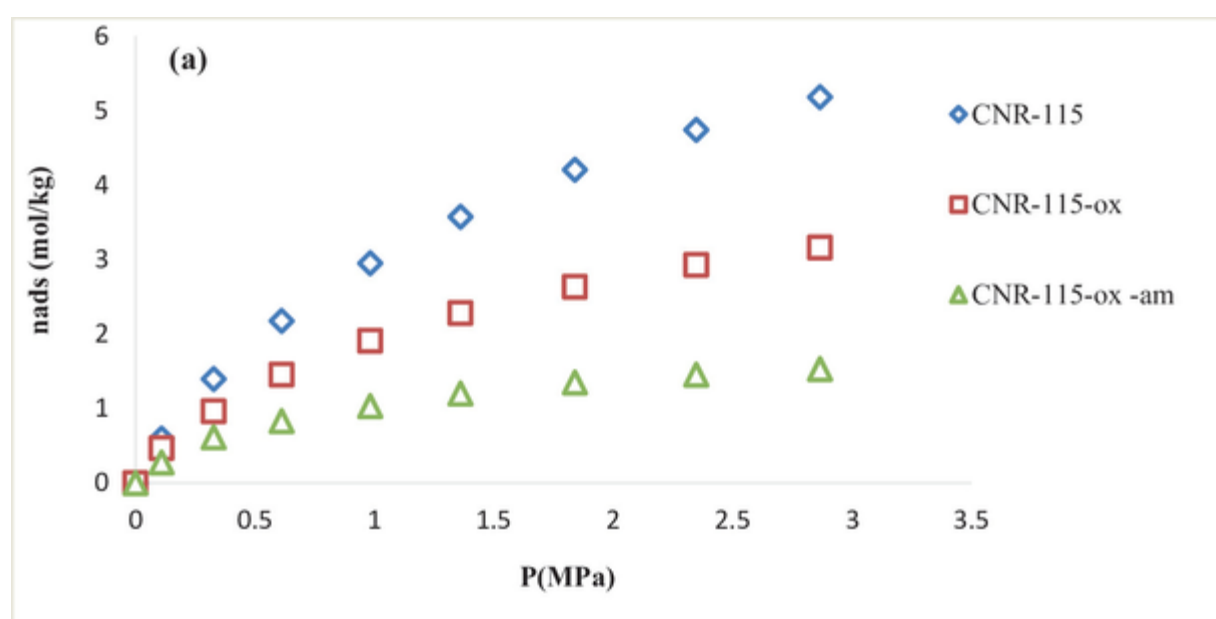
12.3. Results and Discussions

12.3.1. CH_4 and CO_2 Pure Gases Adsorption Isotherm

The Fig. 12.4 shows the results obtained for both CH_4 and CO_2 pure gases adsorption isotherms on CNR-115, CNR-115-ox and CNR-115-ox-am at 303.15 K and the pressure range of 0–3 MPa. The results highlight that, for the pressures ranging from zero to 3 MPa, activated carbons of CNR-115 family present higher adsorption capacities for CO_2 than for CH_4 . Literately, this fact that carbon dioxide is highly adsorbed than methane, agrees with general behavior of activated carbons.

Fig. 12.4

CH_4 (a) and CO_2 (b) pure gases adsorption isotherms on CNR-115, CNR-115-ox and CNR-115-ox-am at 303.15 K



Further possible explanations are based on the difference between CO₂ and CH₄ properties (Table 12.2). From the Table 12.2 it can be seen that; the kinetic diameter of carbon dioxide (330 pm) is less than that of methane (380 pm). When compared to the size of activated carbons of CNR-115 family as previously presented, carbon dioxide (i.e. the one with small size) will tend to be adsorbed than methane (Cui et al. 2004). However, another reason is that, carbon dioxide doesn't present a dipole moment, but it contains unignorable quadrupole moment ($-13.7 \times 10^{40} \text{ cm}^2$), this is contrary to methane which has no dipole or quadrupole moments. The higher the dipole and quadrupole moments, the greater the interactions gas-activated carbon (Rodriguez-Reinoso et al. 1992). In addition, a wider polarizability of CO₂ than CH₄ ($29.1 \times 10^{25} \text{ cm}^2$ of CO₂ > $25.9 \times 10^{25} \text{ cm}^3$ of CH₄) also explains the greatest interactions between CO₂ and activated carbons. Besides, the results also show a significant loss in adsorption capacity for both CH₄ and CO₂ from commercial CNR-115 to modified activated carbons. At 3Mpa, CO₂ adsorption capacity was in the following sequence: CNR-115 ($12.05 \text{ mol kg}^{-1}$) > CNR-115-ox (7.79 mol kg^{-1}) > CNR-115-ox-am (4.05 mol kg^{-1}), and was the same order for CH₄ adsorption capacity: CNR-115 (5.18 mol kg^{-1}) > CNR-115-ox (3.16 mol kg^{-1}) > CNR-115-ox-am (1.53 mol kg^{-1}). The highest CH₄ and CO₂ adsorption capacities of CNR-115 were surely related to its higher BET surface and higher pore volume. Those results were considered as accurate since the errors were very small ($\Delta_{\text{nads}} \leq 1\%$, $\Delta_T \leq 0.5\%$, and $\Delta_p = 1-5\%$).

Table 12.2

Properties of CH₄ and CO₂ molecules (Wu et al. 2015)

Property	CH ₄	CO ₂
Kinetic diameter (pm)	380	330
Dipole moment ($\times 10^{-40} \text{ cm}^2$)	0	0
Quadrupole moment ($\times 10^{-40} \text{ cm}^2$)	0	-13.7
Polarizability ($\times 10^{-25} \text{ cm}^3$)	25.9	29.1

12.3.2. Langmuir Fitting

The Table 12.3 shows the results obtained for the fitting of Langmuir model with CH₄ and CO₂ adsorption isotherms. The maximum Langmuir capacities of (8.45 and $19.26 \text{ mol kg}^{-1}$ for CH₄ and CO₂ respectively) were found to be for unmodified activated carbon (CNR-115). This confirms the relationship between the adsorption capacity and the BET surface area (i.e. the greater the BET surface the higher the adsorption capacity).

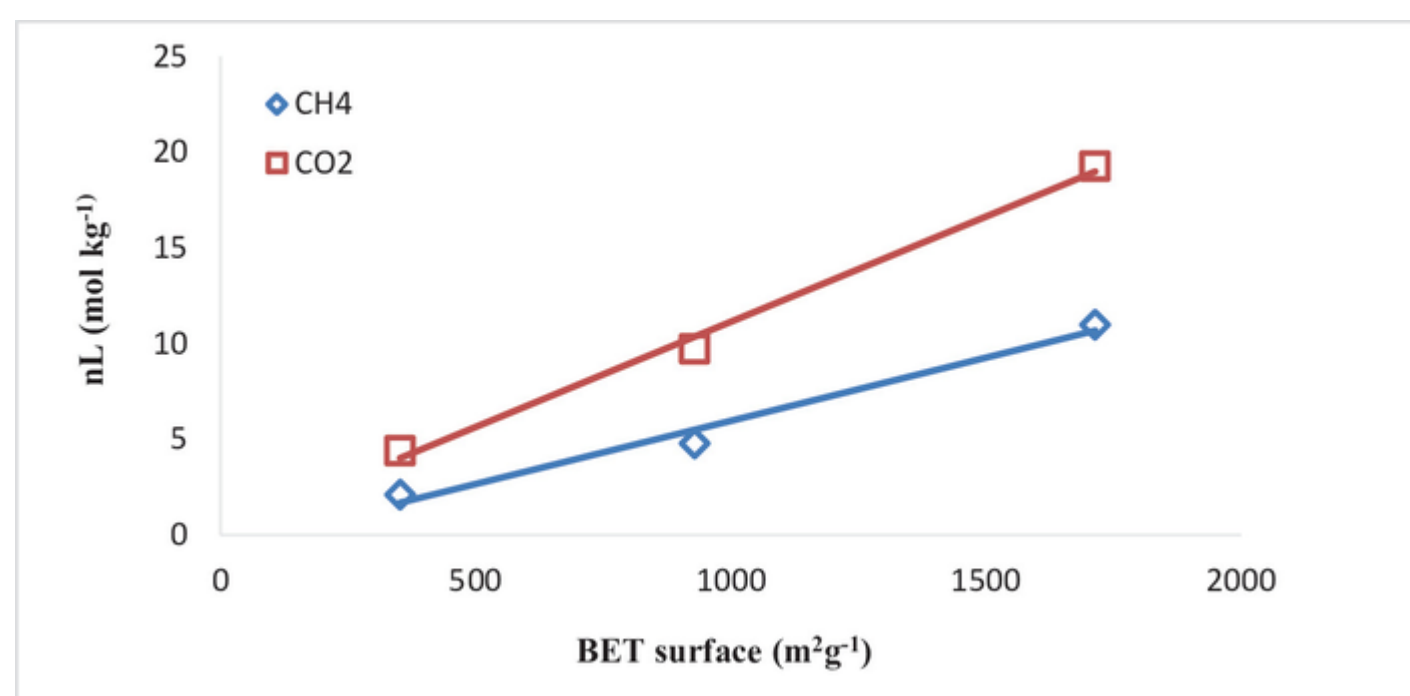
Table 12.3Langmuir parameters of CH₄ and CO₂ on activated carbons of CNR-115 family at 303.15 K

Sample	Components	n_L (mol kg ⁻¹)	P_L (MPa)	Δ_n
CNR-115	CH ₄	8.45	1.79	0.003
	CO ₂	19.26	1.68	0.073
CNR-115-ox	CH ₄	4.78	1.53	0.040
	CO ₂	9.71	0.94	0.120
CNR-115-ox-am	CH ₄	2.10	1.04	0.030
	CO ₂	4.39	0.57	0.010

It can also be observed in Fig. 12.5 that, the maximum Langmuir capacity was in good correlation with BET surface area, with good linear regression ($R_2 \geq 0.98$). However, the results were confirmed as reasonable and reproducible since the fitting error was small ($\Delta_n \leq 0.12$) for all the samples.

Fig. 12.5

Maximum Langmuir capacity versus BET surface area of activated carbons of the CNR-115 family, at 303.15 K



12.3.3. Interesting Side of CNR-115-ox-am: The New Modified Activated Carbon

The results discussed above highlight that CNR-115 adsorbs higher amount of both CH₄ and CO₂ compared to new modified activated carbons (CNR-115-ox and CNR-115-ox-am). However, the adsorption capacity is not the only one performance indicator of an adsorbent. The best one is therefore its selectivity (i.e. capacity to choose one component over another one from the mixture). For CH₄/CO₂ mixtures separation, an activated carbon which adsorbs the least CH₄ and moderated CO₂ can be preferred. This is because, CH₄ as the only one valuable component has to remain in the mixture for further uses (Costa et al. 2020). In this study, the lowest CH₄ adsorption capacity (1.53 mmol/g) was obtained for CNR-115-ox-am, thus the reason to consider it as promising adsorbent for CH₄ enrichment from CH₄/CO₂ mixtures. This was already confirmed by the results of Deneb et al. (Peredo-Mancilla et al. 2018) who studied the adsorption of (CH₄/CO₂ 50:50) mixture on CNR-115, CNR-115-ox and CNR-115-ox-am. According to their results, the selectivity of unmodified CNR-115 (<2.7 through the whole pressure range) was almost 50 times less than the maximum selectivity value (129.0 at 2.17 MPa) for CNR-115-ox-am. Furthermore, when compared to the adsorption capacities from the literature as shown in Table 12.4, methane adsorption capacity obtained in this work for CNR-115-ox-am at 303.15 K and 0.1 MPa (0.27 mol/g), is to the best of our knowledge among the lowest ones that are so far reported for activated carbons. Moreover, adsorption performances of CNR-115-ox-am are comparable to the ones reported for metal organic frameworks like (Cu-MOF) (Wu et al. 2014).

Table 12.4CH₄ and CO₂ pure gases adsorption on different adsorbents, at 0.1 MPa

Adsorbents	Modification process	BET (m ² /g)	T (K)	CH ₄ uptake (mol/kg)	CO ₂ uptake (mol/kg)	Ref.
CNR-115	–	1714	303	0.60	1.38	This work
CNR-115-ox	Air, 400 °C	929	303	0.47	1.18	This work
CNR-115-ox-am	NH ₄ OH, 24 h at 100 °C	352	303	0.27	0.91	This work
GAC	–	865	273	–	4.66	Giraldo et al. (2020)

Adsorbents	Modification process	BET (m ² /g)	T (K)	CH ₄ uptake (mol/kg)	CO ₂ uptake (mol/kg)	Ref.
GACO	HNO ₃ , 6 hat 100 °C	787	273	–	5.38	Giraldo et al. (2020)
GACA	NH ₄ OH, 24 h at 100 °C	634	273	–	7.57	Giraldo et al. (2020)
Pitch-based	–	1457	303	1.10	2.50	Wu et al. (2015)
Cu-MOF	–	105	298	0.47	0.86	Wu et al. (2014)
Cu-MOF	–	105	318	0.35	0.65	Wu et al. (2014)
MOF-1C	–	–	298	0.30	1.50	Bae et al. (2011)

12.4. Conclusion

In this experimental study, CH₄ and CO₂ pure gases adsorption experiments were correctly conducted on commercial and modified activated carbons (family of CNR-115) at 303.15 K and the pressure ranging from zero to three mega Pascals. Adsorption capacity of CO₂ was found to be higher than that of CH₄ for all the three activated carbons of CNR-115 family. A decrease in adsorption capacity was observed for both gases due to the decline in BET surface area and pore blockage which take place during modification process. Experimental isotherms were fitted to Langmuir two-parameter model in order to describe the behavior of adsorption process. Type I isotherm (i.e. monolayer adsorption) was therefore observed for CH₄ and CO₂ adsorption on a set of activated carbon of CNR-115 family. BET surface area was confirmed to be related to the adsorption capacity, and the values obtained are in good agreement with the ones reported in the literature (Peredo-Mancilla et al. 2018; Ho et al. 2021). The modified activated carbon CNR-115-ox-am presents the advantage of adsorbing the least methane than other activated carbons of the CNR-115 family, which is thus the reason to consider this activated carbon as promising adsorbent for the future studies of CH₄ enrichment from CH₄/CO₂ mixtures.

Acknowledgements

The author would like to acknowledge the framework agreement between BIOCAD E₂S of Université de Pau et des Pays de l'Adour (UPPA), CATLP (Communauté d'Agglomération Tarbes-Lourdes-Pyrénées), the French program ANR (ANR-16-IDEX-0002) and CARNOT ISIFOR for their financial support.

References

- Bae Y-S, Hauser BG, Farha OK, Hupp JT, Snurr RQ (2011) Enhancement of CO₂/CH₄ selectivity in metal-organic frameworks containing lithium cations. *Microporous Mesoporous Mater* 141:231–235
- Bessières D, Lafitte T, Daridon J-L, Randzio SL (2005) High pressure thermal expansion of gases: measurements and calibration. *Thermochim Acta* 428:25–30
- Boulinguez B, Le Cloirec P (2015) Purification de biogaz - Élimination des COV et des siloxanes. *Chim Verte*
- Cui A, Bustin RM, Dipple G (2004) Selective transport of CO₂, CH₄, and N₂ in coals: insights from modeling of experimental gas adsorption data. *Fuel* 83:293–303
- da Costa RBR, Valle RM, Hernández JJ, Malaquias ACT, Coronado CJR, Pujatti FJP (2020) Experimental investigation on the potential of biogas/ethanol dual-fuel spark-ignition engine for power generation: combustion, performance and pollutant emission analysis. *Appl Energy* 261:114438
- El-Shafey EI, Ali SNF, Al-Busafi S, Al-Lawati HAJ (2016) Preparation and characterization of surface functionalized activated carbons from date palm leaflets and application for methylene blue removal. *J Environ Chem Eng* 4:2713–2724
- Gasquet V (2020) Epuration d'H₂S du biogaz à partir de résidus de traitement thermique bruts et formulés: Comparaison des performances et compréhension des mécanismes d'adsorption 223
- Giraldo L, Vargas DP, Moreno-Piraján JC (2020) Study of CO₂ adsorption on chemically modified activated carbon with nitric acid and ammonium aqueous. *Front Chem* 8:543452
- Ho BN, Pino-Perez D, Matei Ghimbeu C, Diaz J, Peredo-Mancilla D, Hort C, Bessieres D (2021) Determination of methane, ethane and propane on activated carbons by experimental pressure swing adsorption method. *J Nat Gas Sci Eng* 95:104124
- Jagiello J, Olivier JP (2013) 2D-NLDFT adsorption models for carbon slit-shaped pores with surface energetical heterogeneity and geometrical corrugation. *Carbon Complete* 70–80

- Kapoor R, Ghosh P, Kumar M, Vijay VK (2019) Evaluation of biogas upgrading technologies and future perspectives: a review. *Environ Sci Pollut Res Int* 26:11631–11661
- Madzaki H, KarimGhani WAWAB, Rebitanim NZ, Alias AB (2016) Carbon dioxide adsorption on sawdust biochar. *Procedia Eng* 148:718–725
- Mouahid A, Bessieres D, Plantier F and Pijaudier-Cabot G (2011) A thermostated coupled apparatus for the simultaneous determination of adsorption isotherms and differential enthalpies of adsorption at high pressure and high temperature. *J Therm Anal Calorim*
- Olivier T (2015) Étude technique, Économique et environnementale sur l'injection portée de biométhane dans le réseau de gaz
- Ortiz Cancino OP, Pino Pérez D, Pozo M, Bessieres D (2017) Adsorption of pure CO₂ and a CO₂/CH₄ mixture on a black shale sample: manometry and microcalorimetry measurements. *J Pet Sci Eng* 159:307–313
- Peredo Mancilla JD (2019) Adsorption and separation of carbon dioxide for biomethane production: the use of activated carbons. Thèse de doctorat (Pau)
- Peredo-Mancilla D, Hort C, Jeguirim M, Ghimbeu CM, Limousy L, Bessieres D (2018) Experimental determination of the CH₄ and CO₂ pure gas adsorption isotherms on different activated carbons. *J Chem Eng Data* 63:3027–3034
- Pu Q, Zou J, Wang J, Lu S, Ning P, Huang L, Wang Q (2021) Systematic study of dynamic CO₂ adsorption on activated carbons derived from different biomass. *J Alloys Compd* 887:161406
- Ribeiro R, Sauer T, Lopes F, Moreira R, Grande C, Rodrigues A (2008) Adsorption of CO₂, CH₄ and N₂ in activated carbon honeycomb monolith. *J Chem Eng Data* 53:2311–2317
- Rodriguez-Reinoso F, Molina-Sabio M, Munecas MA (1992) Effect of microporosity and oxygen surface groups of activated carbon in the adsorption of molecules of different polarity. *J Phys Chem* 96:2707–2713
- Rogulska M, Bukrejewski P, Krasuska E (2018) Biomethane as transport fuel (IntechOpen)
- Speight JG (2019) Chapter 15—Hydrogen production. In: Speight JG (ed) *Heavy oil recovery and upgrading*, pp 657–697. Gulf Professional Publishing
- Sun L-M, Meunier F, Brodu N and Manero M-H (2016) Adsorption—aspects théoriques
- Tilagone R, Lecoïnte B (2015) *Gaz naturel—Carburant pour véhicule* 31
- Vondra M, Touš M, Teng SY (2019) Digestate evaporation treatment in biogas plants: a techno-economic assessment by Monte Carlo, neural networks and decision trees. *J Clean Prod* 238:117870
- Wu X, Yuan B, Bao Z, Deng S (2014) Adsorption of carbon dioxide, methane and nitrogen on an ultramicroporous copper metal-organic framework. *J Colloid Interface Sci* 430:78–84
- Wu Y-J, Yang Y, Kong X-M, Li P, Yu J-G, Ribeiro AM, Rodrigues AE (2015) Adsorption of pure and binary CO₂, CH₄, and N₂ gas components on activated carbon beads. *J Chem Eng Data* 60:2684–2693
- Zulkurnai NZ, Md Ali UF, Ibrahim N, Abdul Manan NS (2017) Carbon dioxide (CO₂) adsorption by activated carbon functionalized with deep eutectic solvent (DES). *IOP Conf Ser Mater Sci Eng* 206:012001